Integrated oxy-combustion power generation with carbon capture and humidification–dehumidification desalination cycle

Binash Imteyaz[a,*], Furqan Tahir[b], Dahiru Umar Lawal[c], Kashif Irshad[a], Mohamed Ahmed[a]

[a]Interdisciplinary Research Center for Renewable Energy and Power Systems (IRC-REPS), King Fahd University of Petroleum and Minerals, Dhahran 31261, Saudi Arabia, email: binash.imteyaz@kfupm.edu.sa (B. Imteyaz)
[b]Division of Sustainable Development, College of Science and Engineering, Hamad Bin Khalifa University, Qatar Foundation, Doha, Qatar
[c]Interdisciplinary Research Center for Membranes and Water Security (IRC-MWS), King Fahd University of Petroleum and Minerals, Dhahran, Saudi Arabia

ABSTRACT

The amount of resources devoted to saltwater desalination is substantial and will only rise as the scarcity of water escalates globally. Desalination techniques for seawater, particularly thermal desalination techniques, require a lot of energy and utilize conventional energy sources. The goal of this article is to examine the integration of thermal desalination techniques with carbon capture and sequestration (CCS) power generation. This study utilizes an oxy-combustion-based zero-emission power plant and investigates the performance of a humidification–dehumidification (HDH) cycle integrated with the main cycle. The system constitutes two main cycles, namely (i) oxy-combustion power generation cycle (OPGC) and (ii) humidification–dehumidification (HDH) cycle. The performance of several bottoming cycles coupled with a closed-air-open-water water-heated (CAOW-WH) HDH system is studied to evaluate the thermodynamic feasibility of the system. The effect of top and bottom temperatures of the HDH system and mass flow rates are optimized for gain output ratio (GOR) and recovery rate (RR). A sensitivity analysis of the integrated system was also conducted, and the effect of oxy-combustion operating parameters on the net cycle efficiency was examined. This analysis offers crucial design considerations for such integrated systems to generate power with zero emissions and produces sweet water without additional energy costs.

Keywords: Carbon capture; Desalination; Gain output ratio; Humidification–dehumidification; Oxy-combustion

1. Introduction

Water scarcity has emerged as a pressing global concern affecting nations across the development spectrum [1]. The unprecedented rise in the global population, coupled with rapid industrialization and climate change, has amplified the demand for freshwater resources [2]. Furthermore, the process of urbanization, driven by migration from rural to urban areas, has led to the expansion of cities and increased urban populations. Because of the abundant seawater availability, desalination is considered a reliable option for coastal regions [3,4]. However, desalination is energy intensive and has various environmental concerns involving carbon footprints and brine discharge [5]. The countries in the Gulf region are water scarce, and almost all of their freshwater needs are met by desalination [6,7]. Therefore, there is an urgent need to focus on improving the thermal

* Corresponding author.

efficiency of desalination plants and reducing the associated environmental burdens for sustainable development.

Among desalination technologies, the humidification–dehumidification (HDH) process is an appealing method for small-scale water desalination [8]. It imitates the natural water cycle to produce desalinated water. In this process, a carrier gas, typically air, is exposed to warm seawater to become humidified [9]. The humid air is then directed into a condenser (dehumidifier), where water vapor condenses on the outer surface of tubes as cold seawater flows inside them. HDH is a straightforward technology that replicates nature's water cycle and has the ability to operate using low-grade energy sources like solar energy or waste heat.

The thermal desalination technology utilizes lower grade heat sources, and therefore, it is usually connected to a power plant, waste heat recovery, or renewables [10]. Oxy-combustion carbon capture is a technology designed to mitigate greenhouse gas emissions, particularly carbon dioxide (CO_2), from power plants and industrial facilities that burn fossil fuels [11,12]. It is a carbon capture and storage (CCS) method that involves burning fuel with pure oxygen instead of air, resulting in a flue gas predominantly composed of CO_2 and water vapor [13]. The primary advantage of oxy-combustion carbon capture is that it produces a flue gas stream with a high concentration of CO_2, simplifying the separation and capture process [14,15]. However, it also has some drawbacks, including the need for a significant amount of pure oxygen, which can increase operational costs and energy requirements [16]. The flue gases from the oxy-combustion power plant can be utilized as the heat source for desalination systems.

Several researchers have investigated the room for improvements in the desalination system and its integration with carbon capture. In one study by Bolea et al. [17], the integration of a coal-based power plant equipped with carbon capture and multi-effect desalination (MED) plant was modeled and examined. They considered five scenarios for steam supply from the power plant cycle to the desalination cycle. It was found that the carbon footprints are significantly lowered to desalinate seawater when compared with the power plant without carbon capture. In another study [18], the HDH desalination process with an adsorption heat pump was optimized in terms of thermodynamics and techno economics. They employed an Engineering Equation Solver (EES) for their mathematical model and optimization. Their findings showed that the highest exergy destruction exists in the humidifier, dehumidifier, and absorber. Furthermore, the gain output ratio (GOR) can be substantially improved by increasing the top temperature and compression ratio.

For maximizing the desalinated water output with zero brine discharge, Tahir et al. [5] used the HDH system as the bottom cycle of the MED plant that utilizes the rejected brine, and part of it is desalinated to improve water productivity. The concentrated brine from the HDH is sent to the crystallizer to recover all of the freshwater. They found that the integration of HDH reduces the burden of the crystallizer hence improving thermal efficiency. The optimized value of specific energy consumption was found to be 720 kJ/kg. Zak et al. [19] analyzed the coupling of an oxy-combustion power plant with a MED unit. In their work, they considered MED with and without thermal vapor compression (TVC), and conducted thermal and techno-economic analysis. The detailed modeling was carried out in ASPEN Plus. For their carbon capture power cycle, they employed ion transport membranes (ITMs) for oxygen separation from air. Two power cycles were modeled with different levels of carbon separation capacities (72% and 100%). Their results showed that the oxy-combustion power plant with 100% carbon capture integrated with MED-TVC needs 16% lower CAPEX than that of a plant with 72% carbon capture. In a similar study by Ghorbani et al. [20], a hybrid system consisting of an oxyfuel power plant with carbon capture, CO_2 liquefaction, natural gas liquefaction, and desalination plant was modeled, assessed, and analyzed. They conducted a sensitivity analysis for several operating conditions. It was concluded that increasing the natural gas mass flow rate up to 50% results in higher thermal efficiency and higher freshwater production.

In a recent study by Khani et al. [21], a polygeneration system comprising of carbon capture, solar energy, HDH desalination, and organic Rankine cycle for power generation was examined. The mathematical model was solved in MATLAB software. According to the findings, the incorporation of solar energy enhanced the power generation of the organic Rankine cycle system, increasing it from 37.3% during winter to 59.41% in the summer. Additionally, compared to the base case scenario, the overall power production rises by 18 kW. Finally, the estimated system revenues amount to $50,000 /y, with a payback period of approximately 4.67 y. Studies related to desalination integration with oxy-combustion power plants are still lacking in the literature. For this purpose, the present study focuses on the integration of an oxy-combustion-based zero-emission power plant with the humidification–dehumidification cycle. The system utilizes the heat rejected by flue gas in the oxy-combustion cycle, which is an indispensable step in separating CO_2 and water vapor. The sensitivity analysis is carried out for various operating conditions.

2. System description

2.1. Oxy-combustion power generation cycle

The proposed zero-emission power plant based on the oxy-combustion cycle is shown in Fig. 1. The system consists of a cryogenic air separation unit (ASU), which is a conventional distillation column to separate oxygen from the air. The separated oxygen is compressed at high pressure before it enters the combustion chamber along with the fuel. In order to maintain the desired temperature for the gas turbine material, a portion of the exhaust CO_2 is recycled back into the combustion chamber. The resulting flue gas undergoes expansion in the gas turbine to extract useful work. Additionally, a series of heat exchangers are employed to extract waste heat, which is then utilized to drive a set of steam turbines in the combined cycle power plant.

The flue gas primarily consists of carbon dioxide and water vapor. Through cooling, the flue gas, primarily composed of carbon dioxide and water vapor, undergoes condensation, resulting in a highly-concentrated stream of CO_2. This captured CO_2 is subsequently compressed, with a portion of it being reintroduced into the combustion

chamber, while the remainder is stored for sequestration purposes. It should be noted that as the percentage of recycled CO_2 is increased, the flue gas temperature reduces due to higher dilution of the reacting gases. As the combustion temperature in a pure oxygen environment is immensely high, dilution with recycled CO_2 is necessary to avoid damaging the combustion chamber wall material.

The flue gas exiting the combined cycle power plant still retains a temperature above 200°C, which is typically underutilized in conventional power plants. However, in the oxy-combustion cycle, it becomes essential to cool down the flue gas in order to separate CO_2 from water vapor. Therefore, this innovative system takes advantage of this waste heat to drive the humidification–dehumidification (HDH) cycle, which is utilized for water desalination purposes. By effectively utilizing the waste heat, this system maximizes energy efficiency and contributes to sustainable water desalination processes.

2.2. Humidification–dehumidification cycle

The HDH cycle consists of a humidifier, a dehumidifier, and a water heater, as shown in Fig. 2. The system configuration follows a closed air and open water cycle (CAOW). In the water-heated cycle, seawater is heated between the humidifier and dehumidifier. The dehumidifier tubes (state 4) are filled with cold seawater, which is preheated by absorbing the latent heat of condensation from the humid air leaving the humidifier (state 5). The preheated seawater undergoes further heating through a water heater (states 5–6) before being sprayed on top of the humidifier, where structured-type packing material enhances the surface area for efficient heat and mass transfer. In the air-heated cycle, the seawater is directly sprayed into the humidifier. The air stream leaving the dehumidifier (state 1) becomes humidified as it moves counter currently past the sprayed water in the humidifier (states 2–3). Some of the sprayed water evaporates in the humidifier, while the remaining portion is discharged as brine at the bottom (state 7). The humid air is condensed in the dehumidifier, resulting in the collection of fresh water (state 8).

3. System modeling

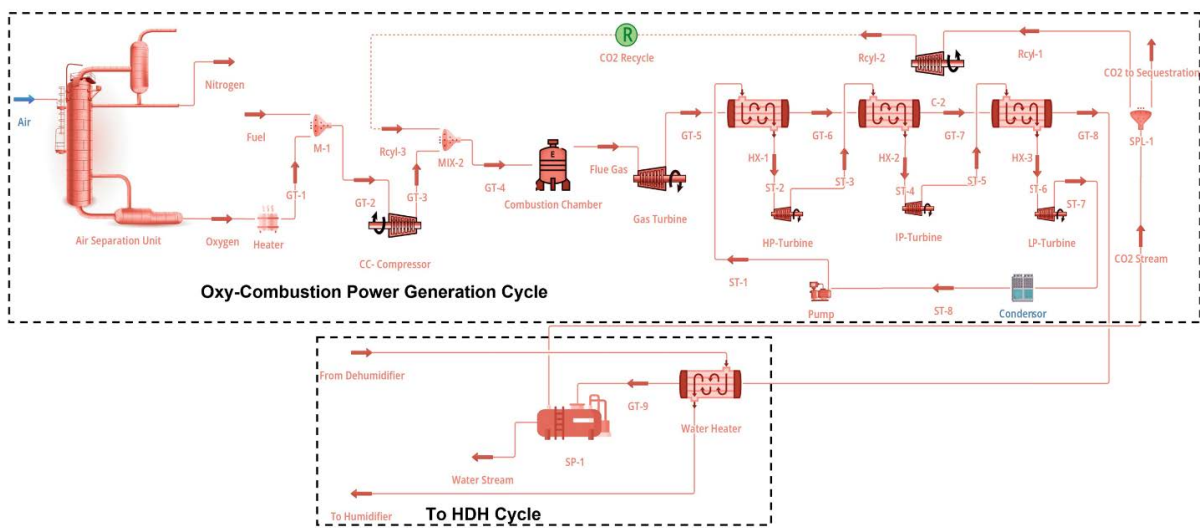This study examines the performance of an oxy-methane combustion power generation system integrated with

Fig. 1. Schematic diagram of the integrated system for zero-emission power generation and sweet water production.
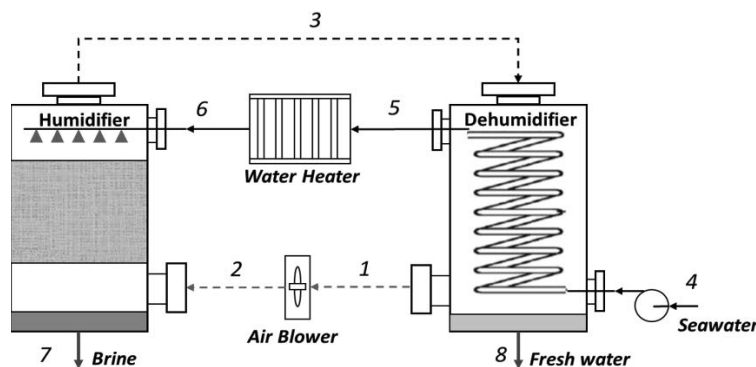

Fig. 2. Schematic diagram of a closed-air open water humidifier dehumidifier desalination system with water heater.

a humidification–dehumidification (HDH) cycle for sweet water production. A combined cycle power plant employing gas and steam turbines is utilized with a fuel consumption of 27.8 kg/s. The percentage recycling of flue gas was varied to study its effect on power generation and HDH systems. All calculations were performed using the commercial software ASPEN HYSYS v11, which has been extensively validated against experimental data [1]. The thermodynamic properties of the gases and mixtures were determined using the Peng–Robinson equation of state.

The steady-state mass and energy governing equations for analyzing the energy of a system can be expressed in the following general format:

$$\sum \dot{m}_{\text{in}} - \sum \dot{m}_{\text{out}} = 0 \tag{1}$$

$$\sum (\dot{m}X)_{\text{out}} = \sum (\dot{m}X)_{\text{in}} \tag{2}$$

To conduct a first law analysis, it is necessary to establish an energy balance across the control volume. This balance can be expressed as follows:

$$\dot{m}_i h_i + \dot{W} + \dot{Q} = \dot{m}_p h_p + \dot{m}_w h_w \tag{3}$$

where $\dot{m}$ represents the flow rate of mass, h represents the specific enthalpy, $\dot{W}$ represents the input power, $\dot{Q}$ represents the rate at which heat is transferred, and the subscripts i, p, and w indicate the inlet, product, and waste gas streams, respectively. The first law efficiency of the power cycle can be given as:

$$\eta_{\text{th}} = \frac{\dot{W}_{\text{useful}}}{\dot{m}_{\text{CH}_4} \times \text{LHV}_{\text{CH}_4}} \tag{4}$$

where $\dot{W}_{\text{useful}}$ is the net useful work obtained from the combined cycle, and LHV_{CH_4} is the lower heating value of methane. The split ratio is defined as the ratio of recycled CO_2 to total carbon dioxide emitted from the combustion process and can be given as:

$$\text{SplitRatio} = \frac{CO_{2,\text{Recycled}}}{CO_{2,\text{Recycled}} + CO_{2,\text{Sequestrated}}} \tag{5}$$

For the humidification cycle, the ratio between the mass flow rate of seawater and the mass flow rate of circulated air is expressed as:

$$m_r = \frac{\dot{m}_w}{\dot{m}_a} \tag{6}$$

Mass balance for the humidifier can be written as:

$$\dot{m}_w - \dot{m}_b = \dot{m}_d \tag{7}$$

While the heat balance equation for the humidifier can be expressed as:

$$\dot{Q}_h = \dot{m}_w \left(h_6 - \frac{\dot{m}_b}{\dot{m}_w} h_7 \right) \tag{8}$$

$$\dot{Q}_h = \dot{m}_a (h_3 - h_2) \tag{9}$$

where $\dot{m}_w$, $\dot{m}_b$, $\dot{m}_a$, $\dot{m}_d$ are the mass flow rates of water, brine, air, and distillate, respectively. h denote the specific enthalpy of the component. Similarly, heat and mass balance for the dehumidifier can be written as:

$$\dot{m}_d = \dot{m}_a (\omega_3 - \omega_2) \tag{10}$$

$$\dot{Q}_d = \dot{m}_w (h_5 - h_4) \tag{11}$$

$$\dot{Q}_d = \dot{m}_a (h_3 - h_2) - \dot{m}_a h_8 \tag{12}$$

where represents the output temperature of the desalinated water, which is considered to be the average temperature of the inlet and outlet air of the dehumidifier. The humidifier and dehumidifier effectiveness is defined as:

$$\varepsilon_h = \max \left(\frac{h_6 - h_7}{h_6 - h_{\text{ideal},7}}, \frac{h_3 - h_2}{h_{\text{ideal},3} - h_2} \right) \tag{13}$$

$$\varepsilon_d = \max \left(\frac{h_5 - h_4}{h_{\text{ideal},5} - h_4 -}, \frac{h_3 - h_2}{h_3 - h_{\text{ideal},2}} \right) \tag{14}$$

where the "ideal, 7" water enthalpy is determined based on the brine's temperature at the inlet air. Similarly, the "ideal, 3" air enthalpy is calculated under fully saturated conditions at the water inlet temperature. Moving on to the dehumidifier, the "ideal, 5" denotes the seawater's outlet enthalpy when its temperature matches the dry bulb temperature of the inlet air. On the other hand, "ideal, 2" represents the air outlet condition for saturated air at the inlet seawater temperature.

The gain output ratio refers to the ratio of the freshwater output gained through the desalination process to the energy input required for the process and can be given as:

$$\text{GOR} = \frac{\dot{m}_d h_{\text{fg}}}{\dot{Q}_m} \tag{15}$$

It is a measure of the efficiency or effectiveness of the thermal desalination system in converting energy input into freshwater output. A higher gain-output ratio indicates a more efficient system where more freshwater is produced for a given amount of energy input.

The above equations are solved using an Engineering Equation Solver (EES) [19], which accounts for the changes in thermal properties of the fluids with operating parameters such as temperature, pressure, etc. EES employs a numerical iterative method to solve this set of equations, achieving convergence when the residuals reach a value below 10^{-6}.

4. Results and discussion

The effect of the mass flow ratio and top humidifier temperature on GOR is shown in Fig. 3. As the water mass flow rate increases, the air absorbs more vapors in

the humidifier resulting in higher distillate; hence GOR increase. However, the GOR rises to a certain point and starts decreasing. As the preheating of seawater in the dehumidifier becomes lower, more heat input is required in the water heater to keep the same humidifier maximum temperature. The rise in distillate production is not the same as the rise in heat input in the water heater, which causes the GOR to decrease. Furthermore, a rise in the top humidifier temperature has a negative effect on the maximum GOR. For a higher humidifier temperature, more heat input is required in the water heater that does not result in the rise of distillate with the same magnitude; hence results in lower GOR. The higher top humidifier temperature does not result in higher GOR; however, it gives more stability of GOR for the broad range of mass flow ratios. In addition, it can be seen that the maximum GOR is obtained at a mass flow ratio of around 2.5 at 70°C top humidifier temperature. Therefore, this optimum mass flow ratio is chosen for further calculations.

The effects of the CO_2 split ratio on the flue gas temperature and mass flow rate are exhibited in Fig. 4. As the dilution increases corresponding to a higher split ratio, the flue gas temperature decreases linearly; however, the total mass flow rate of the flue gas increases rapidly.
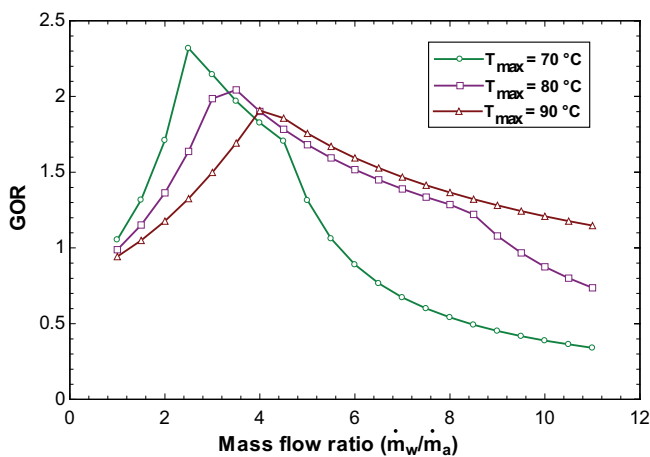
Increasing the split ratio from 0.9 to 0.95 causes the mass flow to approximately double and the flue gas temperature to decrease from 1,456°C to 938°C. This is because the heat capacity of carbon dioxide increases with increasing temperature. Thus, at lower split ratios, which corresponds to higher flue gas temperature, a lower mass rate flow rate can accommodate for the same temperature difference as compared to that of at the higher split ratios.

As the split ratio affects the flue gas temperature and mass flow rate, this also changes the operating condition across the water heater resulting in variation in distillate production. Fig. 5 represents such variation of sweet water production with split ratio and top humidifier temperature. It can be seen that the sweet water production increases with increasing split ratio, although the flue gas temperature decreases. However, the decrease in flue gas temperature is outstripped by the rise in its mass flow rate and hence total heat input. Higher sweet water production is observed at lower top humidifier temperatures. Fig. 6 shows the relationship between the split ratio and heat transfer rate for different top humidifier temperatures. It can be observed that the heat transfer rate increases with
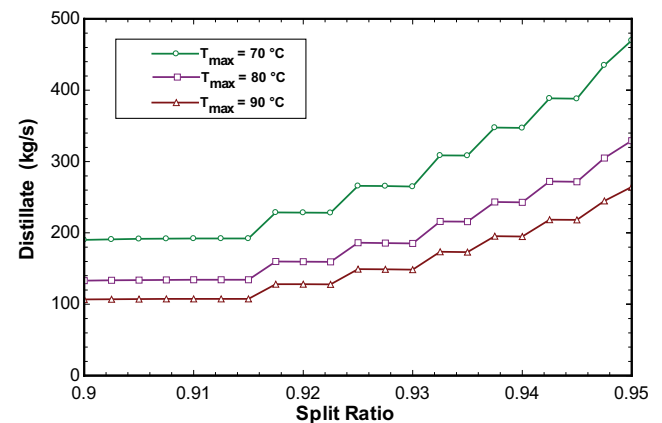

Fig. 3. Effect of mass flow ratio on the gain output ratio.

Fig. 5. Sweet water production rate at various top humidifier temperatures with split ratios.

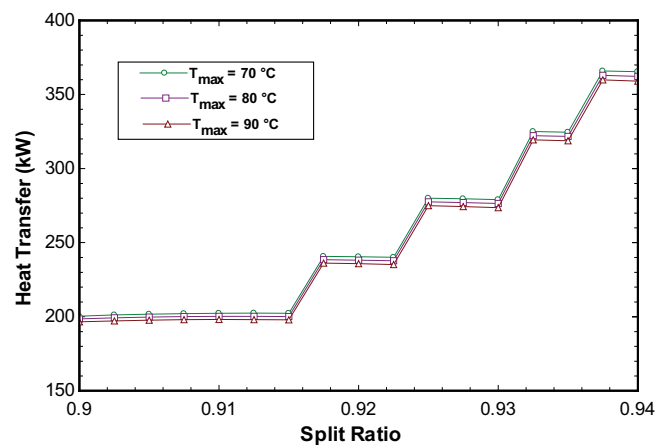Fig. 4. Flue gas temperature and mass flow rate with change in a split ratio.

Fig. 6. Heat transfer rate as a function of split ratio at different top humidifier temperatures.
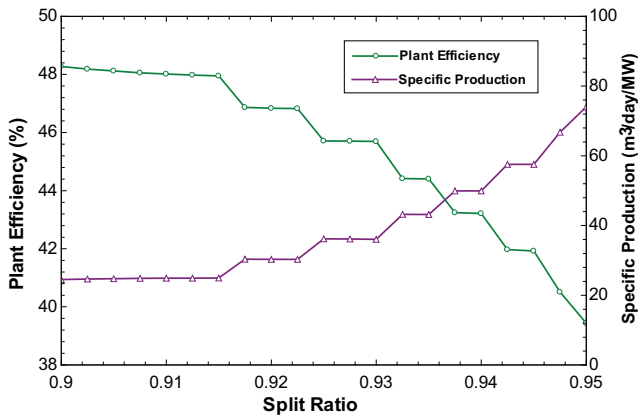
Fig. 7. Oxy-combustion power plant efficiency and specific sweet water production of the HDH system as a function of split ratio (top humidifier temperature = 70°C).

Fig. 8. GOR and recovery ratio of the HDH system at various top humidifier temperatures.

decreasing top humidifier temperature, and increasing the split ratio from 0.9 to 0.94 results in a 75% increase in the heat transfer rate. This is because flue gas temperature remains fixed at a particular split ratio. Therefore, increasing the humidifier temperature decreases the temperature gradient of the water heater, lowering the total heat transfer. This results in lower sweet water production at higher top humidifier temperatures.

At higher split ratios, the heat transfer rate and sweet water production are better, but it also affects the plant efficiency and distillate per unit power output, which is presented in Fig. 7. These results are obtained for the fixed top humidifier temperature of 70°C. The oxy-combustion power plant thermal efficiency decreases with an increasing split ratio as the operating temperature of the combined cycle decreases. An increase in the split ratio from 0.9 to 0.95 results in the plant efficiency from 48.3% to 39.8%, which is a tremendous decrease in overall plant efficiency of 8.5%. While due to enhanced heat transfer, specific sweet water production increases with the split ratio. The specific distillate production per MW power output increases from 27 to 74 m³/d/MW, a rise of 174%, when the split ratio is changed from 0.9 to 0.95. This shows that the higher specific production rate comes at the expense of plant efficiency, and hence, an optimal compromise should be made while designing the integrated system.

Finally, the GOR and recovery ratio (RR) of the HDH system at various top humidifier temperatures is displayed in Fig. 8. Higher GOR and RR benefit the desalination plant, as higher GOR depicts higher productivity, and higher RR shows that lower seawater needs to be circulated for the unit distillate production. In the present case, the GOR decreases with increasing top humidifier temperature due to lower heat transfer. In addition, a higher recovery ratio is observed at higher top humidifier temperatures, although the sweet water production decreases. When the top humidifier temperature is increased from 70°C to 90°C, the RR changes from 5% to 6.2%, showing an increase of 24%. However, due to lower GOR at 90°C, this top humidifier temperature is not optimum for the plant operation.
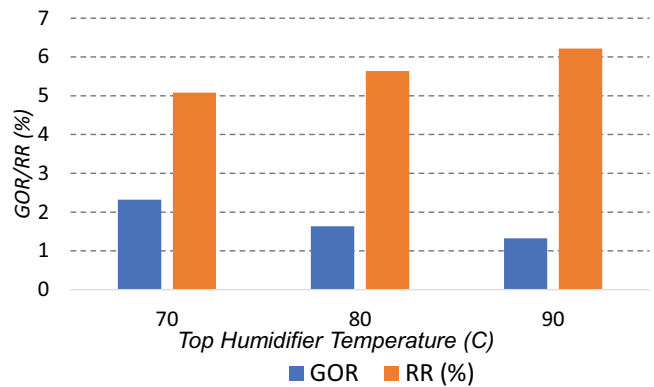
5. Conclusions

This study presents a comprehensive investigation into the performance of an oxy-combustion-based zero-emission power plant integrated with a humidification–dehumidification (HDH) cycle. The system consists of two main cycles: the oxy-combustion power generation cycle (OPGC) and the humidification–dehumidification (HDH) cycle. The thermodynamic feasibility of the integrated system was assessed through the evaluation of various bottoming cycles coupled with the closed-air-open-water water water-heated (CAOW-WH) HDH system. The optimization of the top and bottom temperatures of the HDH system, as well as the mass flow rates, was conducted to maximize the gain output ratio (GOR) and recovery rate (RR) of the system. Additionally, sensitivity analysis was carried out to explore the impact of oxy-combustion operating parameters on the net cycle efficiency. Some of the key findings are as follows:

- The maximum GOR is obtained at a mass flow ratio of 2.5 at 70°C top humidifier temperature.
- Increasing the split ratio from 0.9 to 0.95 causes the mass flow to approximately double and the flue gas temperature to decrease from 1,456°C to 938°C.
- As the split ratio affects the flue gas temperature and mass flow rate, this also changes the distillate production.
- The sweet water production increases with increasing split ratio, although the flue gas temperature decreases.
- The heat transfer rate increases with decreasing top humidifier temperature, and increasing the split ratio from 0.9 to 0.94 results in a 75% increase in the heat transfer rate.
- At higher split ratios, the heat transfer rate and sweet water production are better, but it also affects the plant efficiency and distillate per unit power output.
- An increase in the split ratio from 0.9 to 0.95 results in the plant efficiency from 48.3% to 39.8%, which is a tremendous decrease in overall plant efficiency of 8.5%.
- The specific distillate production per MW power output increases from 27 m³/d/MW to 74 m³/d/MW, a rise of 174%, when the split ratio is changed from 0.9 to 0.95.

- When the top humidifier temperature is increased from 70°C to 90°C, the RR changes from 5% to 6.2%, showing an increase of 24%. However, due to lower GOR at 90°C, this top humidifier temperature is not optimum for the plant operation.

The findings from this analysis offer valuable insights and design considerations for the implementation of integrated systems capable of generating power with zero emissions while producing sweet water without incurring additional energy costs. By leveraging oxy-combustion technology and optimizing the HDH cycle, this integrated approach displays a promising pathway toward sustainable power generation and water resource management. It underscores the potential of such systems to address environmental challenges and contribute to a cleaner and more resilient energy future.

Conflict of interest

The authors declare that they have no known competing financial interests or personal relationships that could have appeared to influence the work reported in this paper.

References

[1] X. Liu, W. Liu, Q. Tang, B. Liu, Y. Wada, H. Yang, Global agricultural water scarcity assessment incorporating blue and green water availability under future climate change, Earth's Future, 10 (2022), doi: 10.1029/2021EF002567.
[2] F. Tahir, A.A.B. Baloch, H. Ali, Resilience of Desalination Plants for Sustainable Water Supply in Middle East, P. Khaiter, M. Erechtchoukova, Eds., Sustainability Perspectives: Science, Policy and Practice, Strategies for Sustainability, Springer, Cham, 2020. Available at: https://doi.org/10.1007/978-3-030-19550-2_15
[3] A.E. Khalifa, B.A. Imteyaz, D.U. Lawal, M.A. Abido, Heuristic optimization techniques for air gap membrane distillation system, Arabian J. Sci. Eng., 42 (2017) 1951–1965.
[4] M. Alhaj, F. Tahir, S.G. Al-Ghamdi, Life-cycle environmental assessment of solar-driven multi-effect desalination (MED) plant, Desalination, 524 (2022) 115451, doi: 10.1016/j.desal.2021.115451.
[5] F. Tahir, S.G. Al-Ghamdi, Integrated MED and HDH desalination systems for an energy-efficient zero liquid discharge (ZLD) system, Energy Rep., 8 (2022) 29–34.
[6] F. Tahir, A. Mabrouk, S.G. Al-Ghamdi, I. Krupa, T. Sedlacek, A. Abdala, M. Koc, Sustainability assessment and techno-economic analysis of thermally enhanced polymer tube for multi-effect distillation (MED) technology, Polymers (Basel), 13 (2021) 681, doi: 10.3390/polym13050681.
[7] D. Lawal, M. Abdul Azeem, A. Khalifa, W. Falath, T. Baroud, M. Antar, Performance improvement of an air gap membrane distillation process with rotating fan, Appl. Therm. Eng., 204 (2022) 117964, doi: 10.1016/j.applthermaleng.2021.117964.
[8] J.S. Shaikh, S. Ismail, A review on recent technological advancements in humidification–dehumidification (HDH) desalination, J. Environ. Chem. Eng., 10 (2022) 108890, doi: 10.1016/j.jece.2022.108890.
[9] M.A. Elhashimi, M. Gee, B. Abbasi, Unconventional desalination: the use of cyclone separators in HDH desalination to achieve zero liquid discharge, Desalination, 539 (2022) 115932, doi: 10.1016/j.desal.2022.115932.
[10] R. Santosh, H.-S. Lee, Y.-D. Kim, A comprehensive review on humidifiers and dehumidifiers in solar and low-grade waste heat powered humidification–dehumidification desalination systems, J. Cleaner Prod., 347 (2022) 131300, doi: 10.1016/j.jclepro.2022.131300.
[11] M.A. Habib, B. Imteyaz, M.A. Nemitallah, Second law analysis of premixed and non-premixed oxyfuel combustion cycles utilizing oxygen separation membranes, Appl. Energy, 259 (2020) 114213, doi: 10.1016/j.apenergy.2019.114213.
[12] B. Imteyaz, F. Tahir, M.A. Habib, Thermodynamic assessment of membrane-assisted premixed and non-premixed oxyfuel combustion power cycles, J. Energy Resour. Technol., 143 (2021), doi: 10.1115/1.4049463.
[13] B. Imteyaz, M.A. Habib, R. Ben-Mansour, The characteristics of oxycombustion of liquid fuel in a typical water-tube boiler, Energy Fuels, 31 (2017) 6305–6313.
[14] F. Tahir, B. Imteyaz, M. Yasir, S.G. Al-Ghamdi, Oxy-methane combustion characteristics in a vertical porous plate reactor, Energy Rep., 9 (2023) 2900–2910.
[15] A.K. Sleiti, W.A. Al-Ammari, L. Vesely, J.S. Kapat, Thermoeconomic and optimization analyses of direct oxy-combustion supercritical carbon dioxide power cycles with dry and wet cooling, Energy Convers. Manage., 245 (2021) 114607, doi: 10.1016/j.enconman.2021.114607.
[16] F. Tahir, H. Ali, A.A.B. Baloch, Y. Jamil, Performance analysis of air and oxyfuel laminar combustion in a porous plate reactor, Energies, 12 (2019) 1706, doi: 10.3390/en12091706.
[17] I. Bolea, J. Uche, L.M. Romeo, Integration of MED with captured CO_2 flue gas compression, Desal. Water Treat., 7 (2009) 124–131.
[18] H. Rostamzadeh, A.S. Namin, H. Ghaebi, M. Amidpour, Performance assessment and optimization of a humidification–dehumidification (HDH) system driven by absorption-compression heat pump cycle, Desalination, 447 (2018) 84–101.
[19] G.M. Zak, N.D. Mancini, A. Mitsos, Integration of thermal desalination methods with membrane-based oxy-combustion power cycles, Desalination, 311 (2013) 137–149.
[20] B. Ghorbani, M. Mehrpooya, H. Ghasemzadeh, Investigation of a hybrid water desalination, oxyfuel power generation and CO_2 liquefaction process, Energy, 158 (2018) 1105–1119.
[21] N. Khani, M.H. Khoshgoftar Manesh, V.C. Onishi, 6E analyses of a new solar energy-driven polygeneration system integrating CO_2 capture, organic Rankine cycle, and humidification–dehumidification desalination, J. Cleaner Prod., 379 (2022) 134478, doi: 10.1016/j.jclepro.2022.134478.